Journal of Environmental Chemical Engineering 11 (2023) 111391

Contents lists available at ScienceDirect

Journal of Environmental Chemical Engineering

journal homepage: www.elsevier.com/locate/jece

Humic acids as complexing agents to drive photo-Fenton at mild pH in saline matrices: Process performance and mechanistic studies

I. Vallés [a], L. Santos Juanes [a], A.M. Amat [a], D. Palma [b], E. Laurenti [b], A. Bianco Prevot [b], A. Arques [a,*]

[a] Grupo de Procesos de Oxidación Avanzada, Departamento de Ingeniería Textil y Papelera, Universitat Politècnica de València, 03001 Alcoy, Spain
[b] Dipartimento di Chimica, Università di Torino, 10125 Torino, Italy

ARTICLE INFO

Editor: Luigi Rizzo

Keywords:
Photo-Fenton
Humic acids
Chlorides
Complexation
EPR

ABSTRACT

The role of iron complexation on (photo)-Fenton process at mild pH has been investigated; in particular, the effect of humic acids, their interaction with chlorides and the involvement of the target pollutants has been studied. For this purpose, solutions consisting in mixture of 6 pollutants (acetaminophen, acetamiprid, amoxicillin, caffeine, carbamazepine and clofibric acid) in different matrices (a) distilled water, b) low salinity water (1 $g{\cdot}L^{-1}$ of Cl^-), c) high salinity water (30 $g{\cdot}L^{-1}$ of Cl^-), d) tap water and e) real sea water) have been irradiated with simulated sunlight with and without humic acids (10 mg L^{-1}). The ability of humic acids to complex Fe(III) resulted in an enhancement of pollutants removal as prevented iron inactivation, but in highly saline waters were they were not able to displace completely Cl^- as ligands for Fe(III) and in sea water where other species could also contribute to inhibit photo-Fenton. Furthermore, pollutants with phenolic and/or carboxylic moieties also contribute to keep iron active at pH = 5, most probably by complexation. This is in line with dissolved iron at the end of the experiment and hydrogen peroxide consumption. Electron spin resonance measurements of ·OH show a very good correlation between the radical formation and pollutants removal, indicating that in the presence of complexing agents, generation of ·OH is favoured. These results indicate that HA could be used as auxiliary to apply photo-Fenton in low salinity environments rather than in real seawater.

1. Introduction

Fenton reaction plays a key role in some of the most promising advanced oxidation processes (AOPs) for water treatment. It is based on the ability of iron salts to catalyse the decomposition of hydrogen peroxide into highly reactive species, such as hydroxyl radicals (·OH) [1]. Because of its high oxidation potential and its low selectivity,·OH is able to attack nearly every organic pollutant present in water, and for this reason Fenton has been selected to deal with contaminants that cannot be eliminated by conventional means, such as the contaminants of emerging concern (CECs) [2-4].

Fenton can be described by Eqs. (1) and (2). While Eq. (1), which results in Fe(II) oxidation into Fe(III), is very fast, Eq. (2) is much slower, being the limiting step of the process. Thus, when Fe(II) is employed, higher reaction rates are observed in the early stages of the process, but they decrease as it is oxidized into Fe(III) [5].

$$Fe^{2+} + H_2O_2 \rightarrow Fe^{3+} + {\cdot}OH + OH^- \quad (1)$$

$$Fe^{3+} + H_2O_2 \rightarrow Fe^{2+} + HO_2^{\cdot} + H^+ \quad (2)$$

Thus, alternative pathways for Fe(III) reduction might result in an enhancement of the process. Among them, the most widely explored is irradiation with photons with $\lambda < 500$ nm at acidic medium [6]. At this pH, $Fe(OH)^{2+}$ is formed and, under an irradiation an internal charge transfer occurs, according to Eq. (3). This is the key pathway of photo-Fenton process, which has been reported to be an order of magnitude faster than "dark" Fenton [1].

$$Fe(OH)^{2+} + h\upsilon \rightarrow Fe^{2+} + {\cdot}OH \quad (3)$$

However, the efficiency of photo-Fenton is closely related to the concentration of $Fe(OH)^{2+}$, which in turn depends on the pH of the solution, reaching the highest concentration in distilled water at pH = 2.8, as can be found in literature [7]; as pH increases, species unable to undergo (photo)-Fenton process are formed, namely $Fe(OH)_2^+$ or $Fe(OH)_3$. This has been widely indicated as a major drawback for the real

* Corresponding author.
E-mail address: aarques@txp.upv.es (A. Arques).

https://doi.org/10.1016/j.jece.2023.111391
Received 31 May 2023; Received in revised form 6 October 2023; Accepted 30 October 2023
Available online 2 November 2023

implementation of photo-Fenton process, as acidification of an effluent would be required, followed by a neutralization after the treatment [8]. In order to avoid iron inactivation at mild pH, the mechanism of photo-Fenton might be varied can be varied by adding substances able to complex Fe(III), that might form other photoactive complexes (FeL^{3+}, where the change of the ligand L is omitted) that undergo Eq. (4) [9], thus regenerating Fe(II).

$$FeL^{3+} + h\upsilon \rightarrow Fe^{2+} + L^{\cdot +} \quad (4)$$

Addition of Fe(III) ligands has been used as a strategy for the application of photo-Fenton under milder conditions [10,11]. Some organic compounds have been employed for this purpose, among them carboxylates [12] or ethylenediamine-N,N′-succinic acid (EDDS) [13]; they have even been employed at larger scale as a tertiary treatment to improve the quality of wastewater effluents [14].

Phenols and polyphenols are known to be good ligands for iron. Their ability as complexing agents depends on the substituents attached to the aromatic ring and their relative position [9]. In the case of catechol, an ortho-substituted diphenol, the formation constant was above 10^{20} [15]. In addition, some phenols and polyphenols are able to (photo)-reduce Fe(III) into Fe(II) via an inner sphere electron transfer [16], thus accelerating the (photo)-Fenton process [9,17]. In contrast, other ligands inhibit the performance of photo-Fenton, as it is the case of chlorides. They are able to form the less active $FeCl_2^+$ complex, that generates $Cl_2^{\cdot -}$, which is less reactive than·OH [9,18]; this behaviour is pH dependent and it has been observed that optimum pH for photo-Fenton is shifted towards a value of 3.4 [19] and that a pH = 5, low concentrations of chlorides slightly enhances photo-Fenton [20]. Interestingly, it has been recently demonstrated that diphenols, and in particular catechol, are able to remove the inhibition of chlorides, by displacing them from the coordination sphere of Fe(III) because of its higher formation constant, what is an interesting result for the application of photo-Fenton in highly saline environments.

In this context, the study of the application of humic acids (HA) mild Fenton processes is interesting. HA are natural substances commonly found in aquatic systems and their structure contains functional groups, such as carboxylic acids of phenols that, as stated above, are good at complexing Fe(III). In fact, HA play an important role in the complexation of iron at the values of pH of natural ecosystems [21], and HA-iron complexes are a major reservoir of iron in the oceans [22].

There are several works reporting on the application of humic and humic-like substances as auxiliaries to apply photo-Fenton at mild pH [23–26] and they have been demonstrated to be efficient, non-toxic and resistant to chemical and biological oxidation [23]. Furthermore, as indicated above, they contain phenolic moieties that might be useful to minimize the effect of chlorides in saline matrices. However, as far as we know, the effect of HA has still not been studied in these experimental conditions.

Finally, most pollutants contain in their structures phenolic, carboxylic or nitrogenated moieties and thus, they can behave themselves as iron ligands, also playing an important role in the photo-Fenton process at mild pH that is commonly neglected [27]. For instance, phenolic pollutants have been reported to shift the optimum pH to values close to 4 [28] and, on the other hand, methylisothiazolinone has been demonstrated to form iron complexes that inhibits photo-Fenton [29].

With this background, the goal of this work is to study the effect of humic acids (HA) on photo-Fenton process at mild pH in the presence of chlorides, as well as to investigate the cross effect of different pollutants themselves. For this purpose, six contaminants of emerging concern have been used as target, namely: acetaminophen (ACM), acetamiprid (AMP), amoxicillin (AMX), caffeine (CAF), carbamazepine (CBZ) and clofibric acid (CLF). They have been chosen because they can be ubiquitously found in aqueous bodies and this mixture has been commonly employed to test the efficiency of photo-Fenton processes under different experimental conditions [9,17,23]. Finally, a mechanistic study has been performed using electron spin resonance (EPR) to assess the ability of the Fenton system to generate hydroxyl radicals in different experimental conditions.

2. Material and methods

2.1. Reagents

Acetaminophen, acetamiprid, amoxicillin, caffeine, carbamazepine, clofibric acid and catechol were supplied by Sigma-Aldrich as high-purity grade reagents (>98%). Humic acids, iron(II) sulphate 7-hydrate (>99%), 5,5-Dimethyl-1-pyrroline N-oxide (DMPO) and catechol (CAT) were also supplied by Sigma-Aldrich. Hydrogen peroxide (30% w/v), sulfuric acid (96% w/w), sodium hydroxide (>98%), sodium chloride (>99%) were obtained from PanReac AppliChem. HPLC grade methanol, formic acid and acetonitrile were also supplied by PanReac AppliChem.

2.2. Experimental set-up and reactions

Five different water matrices were used to perform the experiments. Three of them were prepared by adding different amounts of NaCl to Milli Q water: 1) distilled water (DW) containing no NaCl; 2) low salinity-water (LSW), obtained by adding of 1 $g{\cdot}L^{-1}$ of NaCl (0.017 M) to Milli-Q water and 3) high salinity-water (HSW), in which 30 $g{\cdot}L^{-1}$ of NaCl (0.52 M) were added to Milli-Q water. The other two matrices were 4) real sea water (RSW) taken from the Mediterranean Sea at Xeraco beach, located in the East of Spain (pH = 8.0, conductivity = 21.7 mS cm^{-1} and salinity 36.5 g L^{-1} NaCl [20]; b) tap water (TW), whose pH = 7.4, inorganic carbon = 52 mg L^{-1}, conductivity = 510 μS/cm).

In most cases, target solution consisted in a mixture of the six pollutants with an initial concentration of 5 $mg{\cdot}L^{-1}$ each. Despite this concentration is above that commonly found in natural aqueous systems, it was chosen in order to obtain accurate and reliable kinetic data, as indicated in previous works [23]; However, some experiments have been performed with 500 μg L^{-1} of each pollutant to be closer to real concentrations. In the experiments involving one single pollutant, a concentration of 30 $mg{\cdot}L^{-1}$ was employed, in order to ensure a similar total amount of target pollutants, and to keep the ratios of contaminant vs. hydrogen peroxide and iron. When humic acids were needed, 10 $mg{\cdot}L^{-1}$ of this substance were added to the solution (which accounts for ca. 3 mg L^{-1} of dissolved organic carbon); this amount was chosen as previous works showed that this concentration is convenient for photo-Fenton processes at pH = 5 driven in the presence of humic-like substances [23].

In order to perform the photo-Fenton experiments, 5 $mg{\cdot}L^{-1}$ of Fe(II) was employed, added as sulphate salt. The amount of H_2O_2 was in most experiments 146 $mg{\cdot}L^{-1}$; this is the theoretic value of this reagent required to reach complete mineralization of all six pollutants, calculated from the stoichiometry of oxidation reaction, assuming that CO_2, H_2O and inorganic salts are the final products; it was chosen to avoid exhaustion of this reagent and to normalize the amount of oxidant added to the experiments. More details on this procedure can be found elsewhere [9,24]. Half of this amount of peroxide was used in the experiments involving 500 μg L^{-1} of each pollutant.

Experiments were carried out at room temperature in an open glass reactor (5.5 cm diameter, 3.0 cm height), loaded with 50 mL of the solution. Irradiations were performed with a Solar box (CO.FO.ME. GRA., Milano), equipped with a xenon lamp (1500 W), which spectrum closely matches the solar one. The irradiance was 550 W/m^2, 32% of which is below 500 nm, and thus, prone to be absorbed by the active iron species; this accounts for 15×10^3 kJ m^{-3} after 30 min of irradiation. A specific 340 nm filter glass was used to cut all possible radiation below this wavelength. The experimental procedure to perform the tests always followed the same order: in the first step, pollutants were dissolved

in their corresponding water matrix. Once the target solution was prepared, other substances were added when needed: first the humic acids, followed by iron(II); then, the pH was adjusted by dropwise addition of 0.1 mmol·L^{-1} solutions of NaOH or H_2SO_4 to reach the desired initial value; finally hydrogen peroxide was added and immediately irradiation was started. Magnetic stirring was kept throughout the process.

In addition to this, the following control experiments were carried out with the mixture of pollutants at 5 mg L^{-1}: a) hydrogen peroxide (146 mg L^{-1}) in the dark, b) photolysis, c) photolysis in the presence of iron (5 mg L^{-1}) and d) photolysis in the presence of H_2O_2 (146 mg L^{-1}). These experiments resulted in negligible pollutants degradation (Fig. S1).

Most experiments were performed for 30 min; samples were periodically taken in order to determine pollutants concentration. They were diluted 1:0.5 with methanol in order to quench the excess of H_2O_2. Dissolved iron, remaining hydrogen peroxide and pH were also measured at the end of the experiment.

2.3. Analytical measurement

HPLC (Agilent 1200 series) was used to follow pollutants concentration along the reaction. A Prevail Hichrom column (C18-Select; 250 ×4.6 mm; 5 μm) was used as stationary phase. The mobile phase consisted of a mixture of two compounds, acetonitrile (A) and formic acid 10 mM (B) which composition was: i) an isocratic mixture of 10% of A and 90% of B was kept for 2 min ii) a linear gradient was set to reach 100% of B in 24 min and iii) 3 min were needed for re-equilibration to the initial conditions. The device was equipped with a UV–vis detector. Four different wavelengths were used: 210 nm for amoxicillin and caffeine, 215 nm for carbamazepine, 220 nm for clofibric acid and 240 nm for acetaminophen and acetamiprid. Identifications and quantitations were performed by comparison with standards.

The concentration of iron was determined according to the 1,10-phenanthroline standardized spectrometric procedure (ISO 6332:1988). Consumption of hydrogen peroxide was determined according to a modification of the metavanadate method which is described in detail elsewhere [30].

EPR was employed to follow the generation of hydroxyl radicals. Catechol was used as a surrogate of the more complex HA, as it has been described to be among the most active functional groups to drive photo-Fenton processes [8]. Samples were prepared in a 50 mL open glass vessel, which was loaded with solutions containing Fe(II) and hydrogen peroxide and when needed, catechol, in three different matrices, namely DW, LSW and HSW; pH was adjusted to 5. Then, DMPO was added and a sample was taken an introduced into quartz capillary. A X-band Bruker EMX spectrometer equipped with a cylindrical cavity was used to obtain the EPR-spectra of the DMPO-OH adduct in the range between 3470 and 3560 Gauss. The spectrum was recorded after 1 min

3. Results and discussion

3.1. Photo-Fenton removal of six pollutants with humic acids in DW

The photo-Fenton removal of a mixture of the six pollutants was studied at initial pH = 5.0 and 6.0, with and without humic acids. Fig. 1a shows the plot of the relative concentration of pollutants (ΣC/ΣCo) vs. time, were ΣC is the total amount of pollutants at the sampling time and ΣCo the total initial concentration of pollutants. This cumulative values of the mixture of six pollutants are employed in order not to rely on the particular behaviour of each one [9], as will be discussed in Section 3.2. It can be observed a very fast pollutants removal at the early stages of the process in all cases, which is attributable to the reaction of iron (II) with H_2O_2, that is very efficiently at generating·OH (see Eq. (1)). As Fe(II) is consumed, reduction of the formed Fe(III) becomes the limiting step of the process. In the dark, this process is very slow and in agreement with this, Fig. 1b shows that results obtained in the absence of irradiation are

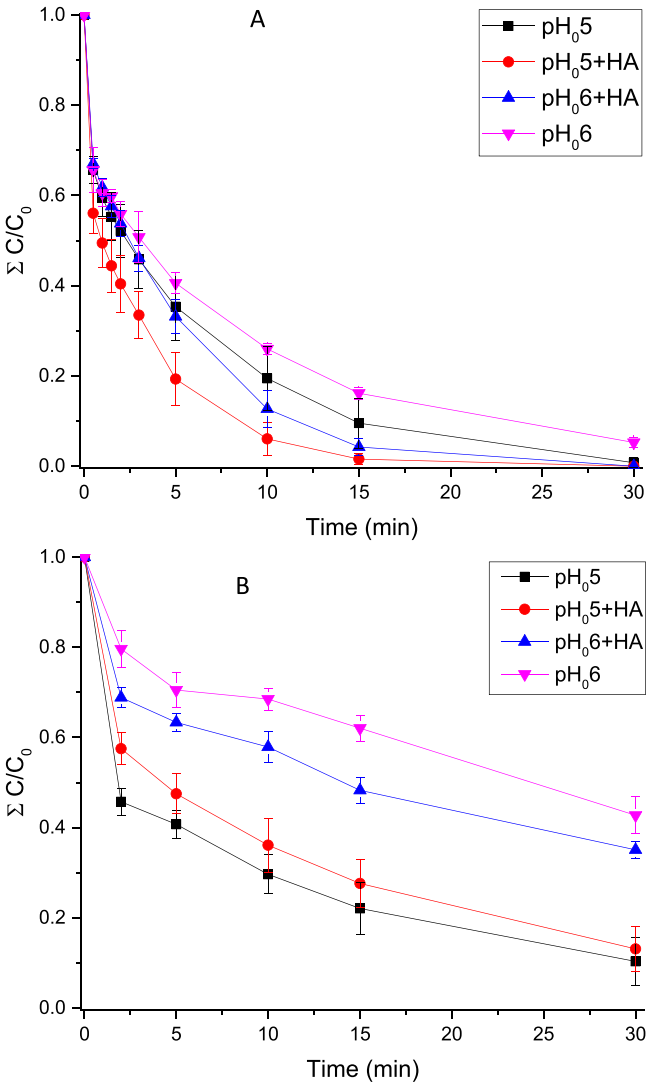

Fig. 1. Plot of the relative concentration of pollutants (ΣC/ΣCo) vs. time in the photo-Fenton (A) and Fenton (B) treatment of a mixture of six pollutants in DW without and with HA (10 mg L^{-1}) at pH = 5 and 6. The initial concentration of each pollutant was 5 mg L^{-1}, the amount of Fe(II) was 5 mg·L^{-1} an the initial concentration of H_2O_2 was 146 mg·L^{-1}.

systematically worse that when solutions are irradiated, and that the decrease of reaction rate along the process is more acute.

Under irradiation, the process occurs either via photolysis of Fe $(OH)^+$ or alternative complexes, in this case Fe-HA. The amount of Fe $(OH)^+$ is strongly dependent of the pH of the medium and it is present in higher amounts at pH = 5 than at pH = 6, thus explaining the order of reactivity [10]. When HA are present, they can form photo-active complexes that regenerates Fe(II) as explained in detail by Ou et al. [31]. The constant for the formation of the Fe(III)-HA complex is reported to be in the order of magnitude of 10^6 at pH = 5, and interestingly, it decreased at higher pH values [32], thus being more likely iron inactivation at pH = 6, in line with the observed trends.

Iron remaining in the solution was measured at the end of the treatment (t = 30 min) and they followed the expected trends; 4.7 mg L^{-1} were measured in the experiment with HA at pH_0 = 5, while this value decreased to 2.5 mg L^{-1} in the absence of these substances. For the at pH_0 = 6 experiments, lower values were found (2.6 mg L^{-1} with HA and 2.0 mg L^{-1} without HA), thus in line with the lower solubility of Fe(III) at this pH and the decreased complexing ability of HA. Finally, a pH decrease was observed in all cases, to reach final values

around 4.

3.2. Effect of the complexing ability of pollutants on the photo-Fenton process

The complexing effect of HA is well established, but pollutants themselves can have a remarkable influence on the process. In order to clarify this point, photo-Fenton was applied in DW at pH = 5 to the mixture of all six pollutants (5 mg L^{-1} each), but also to each contaminant at 30 mg L^{-1} under the same experimental conditions, in parallel experiments. Figs. 2a and 2b show the concentration profile of each pollutant in both series of experiments. Interestingly, very noticeable differences in the reactivity trends could be found among both cases. When all pollutants are together, the observed trend is AMX > CBZ > CLF ≥ CAF ≥ APH > APD while in the parallel removal of the pollutants, it changes to AMX > APH > CLF > > APD > > CAF > CBZ.

Considering that hydroxyl radicals are the key reactive species in the process, pollutants removal would be ruled by the concentration of·OH (which in turn depends on the efficiency of the system to form this species) and the rate constant for the reaction of the pollutant with the·OH, $k_{HO·}$. In the experiment carried out with the mixture of pollutants, the same concentration of·OH for each compound, and hence, their removal can be correlated with the $k_{HO·}$, which can be found in Table 1. In fact, fastest removal was observed for AMX and CBZ, in line with their highest $k_{HO·}$, while APD, with the lowest $k_{HO·}$ wass the most reluctant among the pollutants.

Table 1
Remaining amount of Fe in the solution and hydrogen peroxide consumption after 60 min of photo-Fenton treatment of each single pollutant at an initial concentration of 30 mg L^{-1} in DW at pH = 5. The initial amount of Fe(II) was 5 mg·L^{-1}, the initial concentration of H_2O_2 was 146 mg·L^{-1}. Literature survey of the rate constant for the reaction of each pollutant with hydroxyl radical, $k_{HO·}$ is also provided, together with the corresponding references.

Compound	Disolved Fe (mg L^{-1})	Consumption of H_2O_2 (%)	$K_{HO·}$ ($M^{-1}s^{-1}$) x 10^9	References
AMX	2.3	72	5.4–9.8	[33],[34]
CBZ	0.1	9	8–10.8	[33],[34]
CAF	0.1	11	4.6–6.4	[34],[33]
CLF	2.2	77	5.0–7.6	[33],[34]
APH	2.0	80	2.8–5.8	[34],[33]
APD	1.9	53	2.1–2.3	[35],[34]

On the other hand, in the experiments performed with one single pollutant, the·OH concentration might differ and these differences could be explained by the ability of the pollutants to form (photo)-active complexes with Fe(III), and two groups of compounds can be found. On one side, APH, CLF, AMX and, in a minor extent APD, showed a noticeable degradation and those compounds contain moieties are good at forming active complexes (phenolic or carboxylic groups), or can undergo intermediates with these functional groups after slight oxidation (in the case of APD), as can be seen in Fig. 3. On the other hand, CAF and CBZ, which underwent negligible degradation under those conditions, do not contain phenolic or carboxylic moieties in their structure.

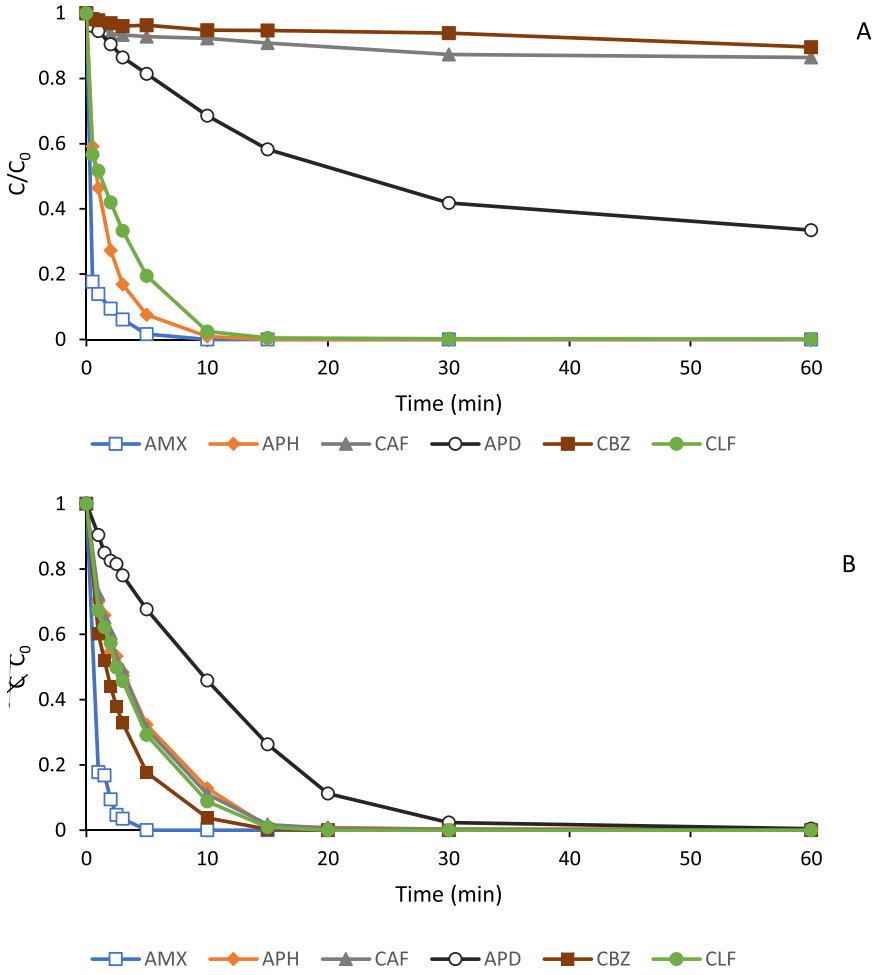

Fig. 2. Plot of the relative pollutants' concentration (C/Co) vs. time obtained for the photo-Fenton treatment of each pollutant (30 mg L^{-1} h) in parallel experiments (A) and the mixture of them (5 mg L^{-1} each) (B). Experiments were carried out in DW at pH = 5, the amount of Fe(II) was 5 mg·L^{-1} an the initial concentration of H_2O_2 was 146 mg·L^{-1}.

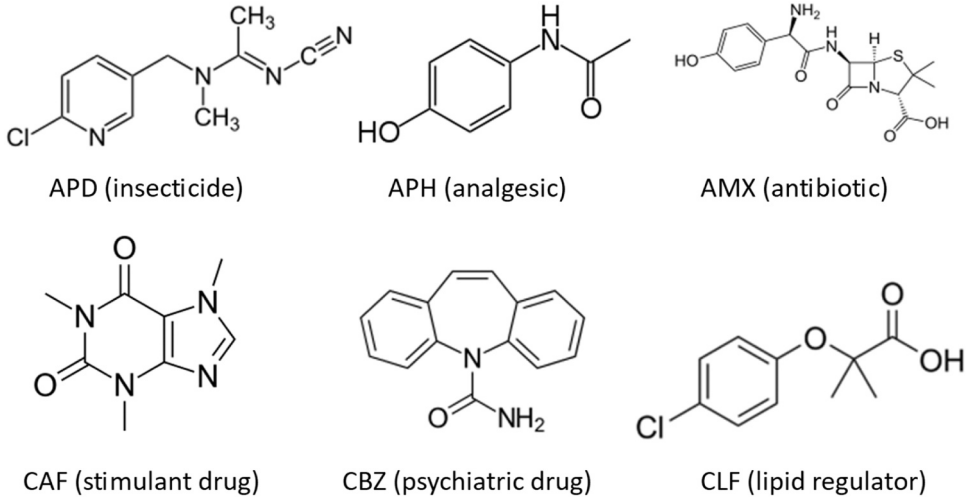

Fig. 3. Chemical structures of the of the target pollutants employed in this work.

The final amount of dissolved iron was consistent iron-complexing ability of AMX, APH, CLF and APD, as the value measured at the end of the reaction was in the range 1.9–2.3 mg L^{-1}, while it was negligible (0.1 mg L^{-1}) for CAF and CBZ. In agreement with this, hydrogen peroxide consumption was very low (ca. 10% of the initial amount) for CAF and CBZ while it was ca. 50% for APD and above 70% in the other cases (see Table 1).

3.3. Combined effect of humic acids and chlorides

The combined effect of the HA as a chelating agent with chlorides on the photo-Fenton process at pH = 5.0 was studied. A series of six different experiments were performed, combining three different concentrations of NaCl, namely 0 g L^{-1} (DW), 1 g L^{-1} (LSW) and 30 g L^{-1} (HSW), with the presence or absence of HA. Results are shown in Fig. 4.

In agreement with previous results with the same mixture of pollutants in the absence of HA and reported elsewhere [9,20], a slight enhancement was observed with LSW when compared with DW, but in HSW some inhibition was observed. This was explained based on Fe(III) speciation: low amounts of Cl^- shifts the highest concentration of Fe $(OH)^+$ from 2.8 towards higher pH values, as described in detail by Millero at el. [7], thus improving the performance of photo-Fenton; however, higher amounts of chlorides results in nearly quantitative formation chlorinated complexes, which undergo the less active $Cl_2^{\bullet-}$ radical, and also the scavenging role of Cl^- for·OH might become significant [9,20].

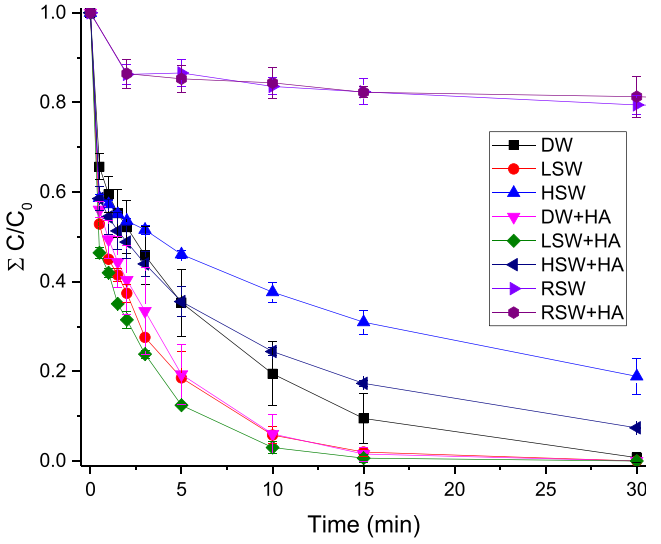

Fig. 4. Plot of the relative concentration of pollutants (ΣC/ΣCo) vs. time without and with HA (10 mg L^{-1}) at pH = 5 in solutions without NaCl (DW), with 1 g L^{-1} of NaCl (LSW), with 30 g L^{-1} of NaCl (HSW) and with real sea water (RSW). The initial concentration of each pollutant was 5 mg L^{-1}, the amount of Fe(II) was 5 mg·L^{-1} an the initial concentration of H_2O_2 was 146 mg·L^{-1}.

Addition of HA was also able to enhance photo-Fenton in all three water matrices. This can be explained by considering that HA is forming photo-active complexes with Fe(III) as stated above. Thus, when HA and Cl^- are in the medium, the higher complexation constant of the first species (ca. 10^6) vs the second one (ca. 10^1) [36] makes that HA partly displaces the Cl^- from the coordination sphere of Fe(III), thus keeping more iron catalytically active. However, as the HA concentration is very low when compared with that of chlorides, in HSW the chlorinated complexes might be predominating, thus explaining that inhibition due to Cl^- is not completely supressed. This is in sharp contrast with the behaviour observed for catechol, which complexation constants with Fe (III) were several order of magnitudes above (ca. 10^{20}), which was able to enhance photo-Fenton even in HSW [9].

Again, in this case dissolved iron and hydrogen peroxide consumption were in agreement with the observed trends. Table 2 shows that systematically, the amount of iron was higher when HS were present than in their absence; however, differences could be found among the different matrices: all iron remained in solution after 30 min when HA were present in DW and HLS matrices (4.6 and 4.7 mg L^{-1}), while this value decreased to 2.5 mg L^{-1} in HSW. Similar trends can be found for hydrogen peroxide consumption, where higher values were reached in

Table 2
Dissolved iron and hydrogen peroxide consumption after 30 min of photo-Fenton treatment of the mixture of 6 pollutants (5 mg L^{-1} each) at pH = 5 in different matrices in the presence and absence of HA (10 mg L^{-1}). In all experiments the initial amount of Fe(II) was 5 mg·L^{-1} an the initial concentration of H_2O_2 was 146 mg·L^{-1}.

Experiment		Disolved Fe (mg L^{-1})	Consumption of H_2O_2 (%)
DW	With HA	4.7	88
	Without HA	2.5	76
LSW	With HA	4.6	83
	Without HA	3.0	73
HSW	With HA	2.5	50
	Without HA	1.6	40
RSW	With HA	1.6	-
	Without HA	0.9	-

the DW and HSW experiments, in particular when HS were present. It is important to remark that in all cases a slight decrease in the pH of the solution was observed, which can be associated to the formation of carboxylic moieties as a result of the oxidation of organic matter. However, in all cases, final pH values were slightly below 4.

A diverging behaviour was observed in experiments carried out with seawater (RSW). Fig. 4 shows that pollutants removal was less than 20%, either with or without HS, and data in Table 2 indicate the final amount of dissolved iron was very low at the end of the process and that hydrogen peroxide consumption was negligible; furthermore, pH remained throughout the process well above 5. All these data show that iron has been completely inactivated and this cannot be only attributed to chlorides, as salinity (36.5 mg L^{-1} of NaCl) was not far away from HSW (30 mg L^{-1} of NaCl). Hence, other species present in the solution strongly interfere the process (e.g carbonates, fluorides) either by complexing iron or by scavenging the generated reaction species. This behaviour has been already observed in a previous work for experiments carried out in the absence of HA [20].

Finally, in order to approach with real situations, experiments were carried out with lower concentration of pollutants (500 μg L^{-1} each). Three different matrices were used, namely DW, TW and RSW; the initial concentrations of iron and HA were kept at 5 mg L^{-1} and 10 mg L^{-1} respectively, but the amount of hydrogen peroxide was decreased to 73 mg L^{-1}. Fig. 5 shows that pollutants removal was very fast in the early stages of the reaction, in agreement with an initial Fenton process driven by Fe(II) and then reaction became slower. It can be observed that in TW some positive effect could be found by HA, and also in DW, although reaction was very fast in this case. On the contrary, HA was not efficient when dealing with RSW.

3.4. EPR measurements

In order to gain further insight into the mechanistic aspects of the reaction, EPR measurements were performed, as the adduct formed between·OH and DMPO gives a very characteristic signal that allows semi-qualitative estimation of the ability of the system to generate·OH, based on the intensity of the signal obtained [37]. Some studies have been performed with humic-like substances showing some ability to form·OH at low concentrations, although at higher concentration

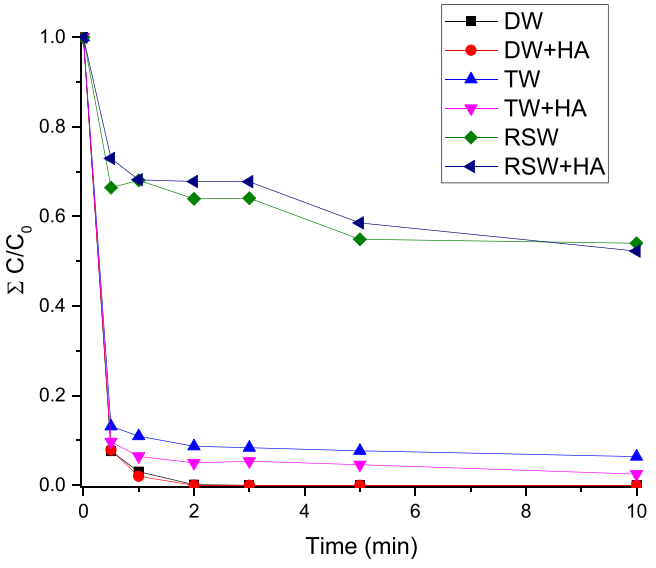

Fig. 5. Plot of the relative concentration of pollutants (ΣC/ΣCo) vs. time without and with HA (10 mg L^{-1}) at pH = 5 in distilled water (DW), tap water (TW), and with real sea water (RSW). The initial concentration of each pollutant was 500 μg L^{-1}, the amount of Fe(II) was 5 mg·L^{-1} an the initial concentration of H_2O_2 was 73 mg·L^{-1}.

predominated the generation of singlet oxygen [38] but signal attributable to the DMPO-OH adduct was much more intense in the presence of iron and hydrogen peroxide, in line with the existence of a (photo)-Fenton-like process [25,39]. However, in order to measure interactions with chlorides, a simpler system has been considered, using catechol as a surrogate for HA, as phenolic groups are among the most active moieties of HA to assist photo-Fenton [9]. Fig. 6 shows that signal generated by the Fenton system in distilled water at pH = 5 in the presence and absence of catechol. This indicates that there is an efficient·OH production with a high signal/noise ratio. However, it can be observed that the signal is more intense in the presence of catechol, which can be related with a better performance of the Fenton system.

Experiments were also performed using LSW and HSW in the presence or absence of CAT. In order to compare data, the signal intensity was calculated as the average of the height of the four distinctive peaks of the DMPO-OH adduct [39]. Fig. 7 shows the signal intensity of hydrogen radicals produced after one minute of the addition of hydrogen peroxide to the reaction mixture. Two clear trends were observed, that are coincident with the efficiency of photo-Fenton reported in previous sections: a) generation of·OH in the presence of complexing agent is always more efficient than it is absence and b) with and without CAT, the formation of·OH in the different matrices followed the order LSW > DW > HSW, confirming that low/moderate amount of chlorides favoured·OH formation, while inhibition was observed at high salinity.

4. Conclusions

HA have been demonstrated as efficient complexing agents to drive photo-Fenton processes at mild pH in aqueous matrices containing chlorides. EPR measurements shown an enhanced production of·OH in the presence of these chelating agents, even in HSW. However, in experiments run with RSW the positive role of HA, most probably to the existence of other interferences, beyond chlorides, whose natures deserves to be investigated.

This is an interesting result for the application of this type of processes in water containing low/moderate salinity, such as irrigation water, where the presence of HS might play to different roles: a) improve the quality of water and b) to fertilize the crops. In particular, experiments carried out with tap water and low concentration of pollutants indicates that this approach is meaningful. However, to assess real applicability it is necessary to perform experiments with real samples and with sunlight at larger scale and also carefully test the effect on crops.

Target pollutants have also been demonstrated to play an important role on photo-Fenton that has been scarcely considered. In this regard, assessing the individual effect of pollutants present in the reaction mixture would be meaningful when exploring the applicability of (photo)-Fenton in different types of effluents. In addition, performing experiments with pollutants that have no ability to complex iron, such as caffeine, as a control when developing new iron-based processes seams interesting.

CRediT authorship contribution statement

I. Vallés: Investigation, Writing – original draft. **L. Santos Juanes:** Formal analysis, Data curation **A.M. Amat:** Funding acquisition, Conceptualization. **D. Palma:** Investigation, Methodology, Writing – review & editing. **E. Laurenti.** Methodology. **A. Bianco Prevot:** Supervision, Funding acquisition. **A. Arques:** Supervision, Writing – review & editing, Conceptualization.

Declaration of Competing Interest

The authors declare the following financial interests/personal relationships which may be considered as potential competing interests:

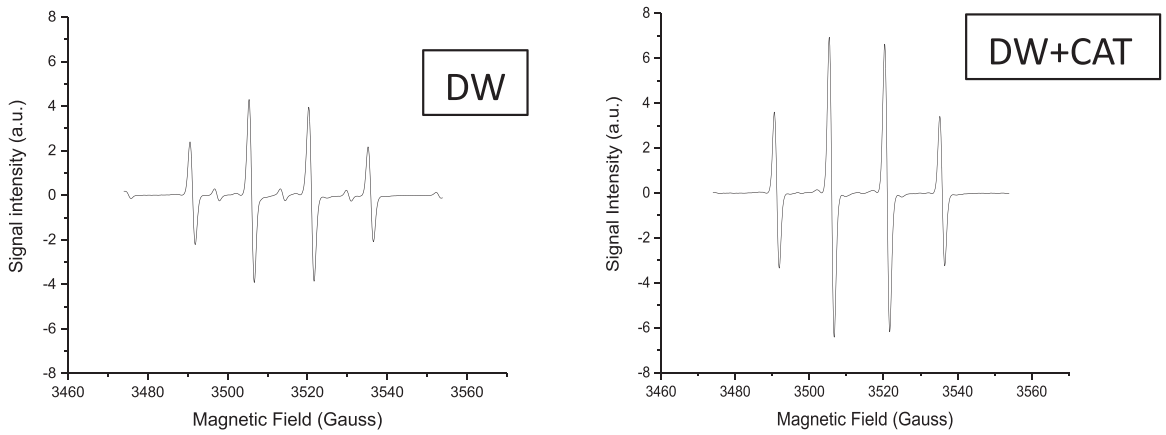

Fig. 6. EPR spectra recorded for the DMPO-OH adduct after 1 min of adding H_2O_2 to the system consisting in DMPO and Fe(II) in distilled water at pH = 5, with and without catechol (CAT).

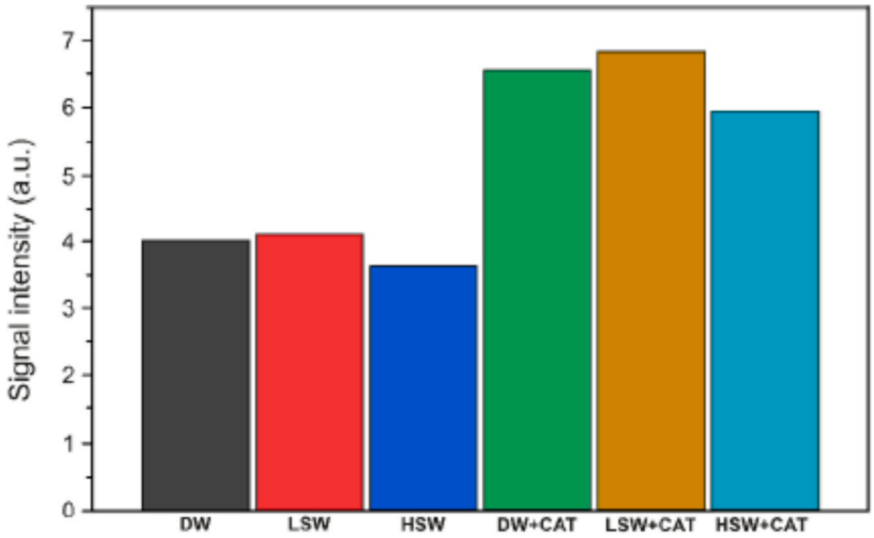

Fig. 7. Signal intensity of the EPR spectra recorded for the DMPO-OH adduct after 1 min of adding H_2O_2 to the system consisting in DMPO and Fe(II) at pH = 5, in DW, LSW and HSW in the presence and absence of CAT.

Antonio Arques reports financial support was provided by European Commission. Antonio Arques reports financial support was provided by Spain Ministry of Science and Innovation.

Data Availability

Data will be made available on request.

Acknowledgements

Authors want to acknowledge the financial support of Spanish Ministerio de Ciencia e Innovación (PID2021-126400OB-C31, AquaEnAgri Project) and TED2021-130994B-C32 (Ecotranseas) funded by European Union NextGenerationEU with the support of Ministerio de Ciencia e Innovación – Spanish Government. Project AGROALNEXT/2022/041, funded by European Union NextGenerationEU (PRTR-C17) with the support of Ministerio de Ciencia e Innovación – Spanish Government and Generalitat Valenciana in also acknowledged. Authors also acknowledge support from the Project CH4.0 under the MUR program "Dipartimenti di Eccellenza 2023–2027" (CUP: D13C22003520001). I. Vallés acknowledges Ministerio de Universidades (FPU21/01336).

Appendix A. Supporting information

Supplementary data associated with this article can be found in the online version at doi:10.1016/j.jece.2023.111391.

References

[1] J.J. Pignatello, E. Oliveros, A. MacKay, Advanced oxidation processes for organic contaminant destruction based on the fenton reaction and related chemistry, Crit. Rev. Environ. Sci. Technol. 36 (2006) 1–84, https://doi.org/10.1080/10643380500326564.

[2] Y. Liu, Y. Zhao, J. Wang, Fenton/Fenton-like processes with in-situ production of hydrogen peroxide/hydroxyl radical for degradation of emerging contaminants: advances and prospects, J. Hazard. Mater. 404 (2021), 124191, https://doi.org/10.1016/j.jhazmat.2020.124191.

[3] L. Rizzo, S. Malato, D. Antakyali, V.G. Beretsou, M.B. Đolić, W. Gernjak, E. Heath, I. Ivancev-Tumbas, P. Karaolia, A.R. Lado Ribeiro, G. Mascolo, C.S. McArdell, H. Schaar, A.M.T. Silva, D. Fatta-Kassinos, Consolidated vs new advanced treatment methods for the removal of contaminants of emerging concern from urban wastewater, Sci. Total Environ. 655 (2019) 986–1008, https://doi.org/10.1016/j.scitotenv.2018.11.265.

[4] M. Liu, Z. Feng, X. Luan, W. Chu, H. Zhao, G. Zhao, Accelerated Fe^{2+} regeneration in an effective electro-Fenton process by boosting internal electron transfer to a nitrogen-conjugated Fe(III) complex, Environ. Sci. Technol. 55 (2021) 6042–6051, https://doi.org/10.1021/acs.est.0c08018.

[5] P. García-Negueroles, S. García-Ballesteros, L. Santos-Juanes, C. Sabater, M. A. Castillo, M.F. López-Pérez, R. Vicente, A.M. Amat, A. Arques, Humic like substances extracted from oil mill wastes in photo-Fenton processes:

Characterization, performance and toxicity assesment, J. Environ. Chem. Eng. 9 (2021), 106862, https://doi.org/10.1016/j.jece.2021.106862.
[6] S. Malato, P. Fernández-Ibáñez, M.I. Maldonado, J. Blanco, W. Gernjak,W, Decontamination and disinfection of water by solar photocatalysis: Recent overview and trends, Catal. Today 147 (2009) 1–59, https://doi.org/10.1016/j.cattod.2009.06.018.
[7] F.J. Millero, W. Yao, J. Aicher, The speciation of Fe(II) and Fe(III) in natural waters, Mar. Chem. 50 (1995) 21–39, https://doi.org/10.1016/0304-4203(95)00024-L.
[8] M. Costamagna, A. Arques, V.G. Lo-Iacono-Ferreira, A. Bianco Prevot, Environmental assessment of solar photo-Fenton processes at mild condition in the presence of waste-derived bio-based substances, Nanomaterials 12 (2022) 2781, https://doi.org/10.3390/nano12162781.
[9] I. Vallés, I. Sciscenko, M. Mora, P. Micó, A.M. Amat, L. Santos-Juanes, J. Moreno-Andrés, A. Arques, On the relevant role of iron complexation for the performance of photo-Fenton process at mild pH: role of ring substitution in phenolic ligand and interaction with halides, Appl. Catal. B: Environ. 331 (2023), 122708, https://doi.org/10.1016/j.apcatb.2023.122708.
[10] L. Santos-Juanes, A.M. Amat, A. Arques, Strategies to drive photo-Fenton process at mild conditions for the removal of xenobiotics from aqueous systems, Curr. Org. Chem. 21 (2017) 1074–1083, https://doi.org/10.2174/1385272821666170102150337.
[11] L. Clarizia, D. Russo, I. Di Somma, R. Marotta, R. Andreozzi, Homogeneous photo-Fenton processes at near neutral pH: a review, Appl. Catal. B: Environ. 209 (2017) 358–371, https://doi.org/10.1016/j.apcatb.2017.03.011.
[12] J.H.O.S. Pereira, D.B. Queirós, A.C. Reis, O.C. Nunes, M.T. Borges, R.A. R. Boaventura, V.J.P. Vilar, Process enhancement at near neutral pH of a homogeneous photo-Fenton reaction using ferricarboxylate complexes: application to oxytetracycline degradation, Chem. Eng. J. 253 (2014) 217–228, https://doi.org/10.1016/j.cej.2014.05.037.
[13] W. Huang, M. Brigante, F. Wu, K. Hanna, G. Mailhot, Development of a new homogenous photo-Fenton process using Fe(III)-EDDS complexes, J. Photochem. Photobiol. A: Chem. 239 (2012) 17–23, https://doi.org/10.1016/j.jphotochem.2012.04.018.
[14] E. Gualda-Alonso, N. Pichel, P. Soriano-Molina, E. Olivares-Ligero, F.X. Cadena-Aponte, A. Agüera, J.A. Sánchez Pérez J.A, J.L. López, Continuous solar photo-Fenton for wastewater reclamation in operational environment at demonstration scale, J. Hazard. Mater. 459 (2023), 132101, https://doi.org/10.1016/j.jhazmat.2023.132101.
[15] N.R. Perron, J.L. Brumaghim, A review of the antioxidant mechanisms of polyphenol compounds related to iron binding, Cell Biochem Biophys. 53 (2009) 75–100, https://doi.org/10.1007/s12013-009-9043-x.
[16] Y. Pan, R. Qin, M. Hou, J. Xue, M. Zhou, L. Xu, Y. Zhang, The interactions of polyphenols with Fe and their application in Fenton/Fenton-like reactions, Sep. Purif. Technol. 300 (2022), 121831, https://doi.org/10.1016/j.seppur.2022.121831.
[17] J. Moreno-Andrés, L. Vallés, P. García-Negueroles, L. Santos-Juanes, A. Arques, Enhancement of iron-based photo-driven processes by the presence of catechol moieties, Catalysts 11 (2021) 372, https://doi.org/10.3390/catal11030372.
[18] J. Bacardit, J. Stoltzner, E. Chamarro, S. Esplugas, Effect of salinity on the photo-Fenton process, Ind. Eng. Chem. Res. 46 (2007) 7615–7619, https://doi.org/10.1021/ie070154o.
[19] A.J. Machulek, J.E. Moraes, C. Vautier-Giongo, C.A. Silverio, L.C. Friedrich, C. A. Nascimento, M.C. Gonzalez, F.H. Quina, Abatement of the inhibitory effect of chloride anions on the photo-Fenton process, Environ. Sci. Technol. 41 (2007) 8459–8463, https://doi.org/10.1021/es071884q.
[20] I. Vallés, L. Santos-Juanes, A.M. Amat, J. Moreno-Andrés, A. Arques, Effect of salinity on UVA-Vis light driven photo-Fenton process at acidic and circumneutral pH, Water 13 (2021) 1315, https://doi.org/10.3390/w13091315.
[21] M. Gledhill, K.N. Buck, The organic complexation of iron in the marine environment: a review, Front. Microbiol 3 (2012) 1–17, https://doi.org/10.3389/fmicb.2012.00069.
[22] E. Årstøl, M.F. Hohmann-Marriott, Cyanobacterial siderophores - physiology, structure, biosynthesis, and applications, Mar. Drugs 17 (2019) 281, https://doi.org/10.3390/md17050281.
[23] J. Gomis, M.G. Gonçalves, R.F. Vercher, C. Sabater, M.A. Castillo, A. Bianco Prevot, A.M. Amat, A. Arques, Determination of photostability, biocompatibility and efficiency as photo-Fenton auxiliaries of three different types of soluble bio-based substances (SBO, Catal. Today 252 (2015) 177–183, https://doi.org/10.1016/j.cattod.2014.10.015.
[24] J. Gomis, L. Carlos, A. Bianco Prevot, A.C.S.C. Teixeira, M. Mora, A.M. Amat, R. Vicente, A. Arques, Bio-based substances from urban waste as auxiliaries for solar photo-Fenton treatment under mild conditions: optimization of operational variables, Catal. Today 240 (2015) 39–45, https://doi.org/10.1016/j.cattod.2014.03.034.
[25] S. García-Ballesteros, P. García-Negueroles, A.M. Amat, A. Arques, Humic-like substances as auxiliaries to enhance advanced oxidation processes, ACS Omega 7 (2022) 3151–3157, https://doi.org/10.1021/acsomega.1c05445.
[26] D. Palma, A. Bianco Prevot, M. Brigante, D. Fabbri, G. Magnacca, C. Richard, G. Mailhot, R. Nisticò, New insights on the photodegradation of caffeine in the presence of bio-based substances-magnetic iron oxide hybrid nanomaterials, Materials 11 (2018) 1084, https://doi.org/10.3390/ma11071084.
[27] R. Yin, Y. Chen, J. Hu, G. Lu, L. Zeng, W. Choi, M. Zhu, Complexes of Fe(III)-organic pollutants that directly activate Fenton-like processes under visible light, Appl. Catal. B: Environ. 283 (2021), 119663, https://doi.org/10.1016/j.apcatb.2020.119663.
[28] S. García-Ballesteros, M. Mora, R. Vicente, C. Sabater, M.A. Castillo, A. Arques, A. M. Amat, Gaining further insight into photo-Fenton treatment of phenolic compounds commonly found in food processing industry, Chem. Eng. J. 288 (2016) 126–136, https://doi.org/10.1016/j.cej.2015.11.031.
[29] V. Duarte-Alvarado, L. Santos-Juanes, A. Arques, A.M. Amat, Mild Fenton processes for the removal of preservatives: Interfering effect of methylisothiazolinone (MIT) on paraben degradation, Catalysts 12 (2022) 1390, https://doi.org/10.3390/catal12111390.
[30] R.F.P. Nogueira, M.C. Oliveira, W.C. Paterlini, Simple and fast spectrophotometric determination of H_2O_2 in photo-Fenton reactions using metavanadate, Talanta 66 (2005) 86–91, https://doi.org/10.1016/j.talanta.2004.10.001.
[31] X. Ou, S. Chen, X. Quan, H. Zhao, Photochemical activity and characterization of the complex of humic acids with iron(III), J. Geochem. Explor 102 (2009) 49–55, https://doi.org/10.1016/j.gexplo.2009.02.003.
[32] S. García Ballesteros, M. Costante, R. Vicente, M. Mora, A.M. Amat, A. Arques, L. Carlos, F.S. García Einschlag, Humic-like substances from urban waste as auxiliaries for photo-Fenton treatment: a fluorescence EEM-PARAFAC study, Photochem. Photobiol. Sci. 16 (2017) 38–45, https://doi.org/10.1039/C6PP00236F.
[33] B.A. Wols, C.H.M. Hofman-Caris, Review of photochemical reaction constants of organic micropollutants required for UV advanced oxidation processes in water, Water Res 46 (2012) 2815–2827, https://doi.org/10.1016/j.watres.2012.03.036.
[34] J. Gomis, A. Bianco Prevot, E. Montoneri, M.C. González, A.M. Amat, D.O. Mártire, A. Arques, L. Carlos, Waste sourced bio-based substances for solar-driven wastewater remediation: Photodegradation of emerging pollutants, Chem. Eng. J. 235 (2014) 236–243, https://doi.org/10.1016/j.cej.2013.09.009.
[35] J.A. Malvestiti, A. Cruz-Alcalde, N. López-Vinent, R.F. Dantas, Carme Sans, Catalytic ozonation by metal ions for municipal wastewater disinfection and simulataneous micropollutants removal, Appl. Catal. B: Environ. 259 (2019), 118104, https://doi.org/10.1016/j.apcatb.2019.118104.
[36] J. De Laat, T.G. Le, Effects of chloride ions on the iron(III)-catalyzed decomposition of hydrogen peroxide and on the efficiency of the Fenton-like oxidation process, Appl. Catal. B: Environ. 66 (2006) 137–146, https://doi.org/10.1016/j.apcatb.2006.03.008.
[37] Y. Hu, Y. Li, J. He, T. Liu, K. Zhang, X. Huang, L. Kong, J. Liu, EDTA-Fe(III) Fenton-like oxidation for the degradation of malachite green, J. Environ. Manag. 226 (2018) 256–263, https://doi.org/10.1016/j.jenvman.2018.08.029.
[38] P. Avetta, F. Bella, A. Bianco Prevot, E. Laurenti, E. Montoneri, A. Arques, L. Carlos, Waste cleaning waste: photodegradation of monochlorophenols in the presence of waste-derived photosensitizer, ACS Sustain. Chem. Eng. 1 (2013) 1545–1550, https://doi.org/10.1021/acsomega.9b02241.
[39] P. García-Negueroles, S. García-Ballesteros, A.M. Amat, E. Laurenti, A. Arques, L. Santos-Juanes. Unveiling the dependence between hydroxyl radical generation and performance of Fenton systems with complexed iron, ACS Omega, 4, 26, 21698–21703. https://doi.org/10.1021/acsomega.9b02241.